Time Series Calibrated Carbon Emissions and Atmospheric Response

© Clifford E. Singer, November 14, 2005
csinger@uiuc.edu
University of Illinois at Urbana-Champaign

This file contains preliminary results for inclusion in the CCSP Workshop electronic poster set collection but not for further reproduction. References to the concepts in this material should cite poster P-CA2.5, U.S. Climate Change Science Program (CCSP) Workshop, “Climate Science in Support of Decisionmaking,,” November 14-16, 2005, Arlington, Virginia. For derivation methods cite T.S. Gopi Rethinaraj, *Modeling Global and Regional Energy Futures,* University of Illinois at Urbana-Champaign PhD Thesis (2005), which can be obtained in electronic form from T. S. Gopi Rethinaraj at <spptsgrc@nus.edu.sg>. For references to detailed results, obtainfrom the first author at cesinger@uiu c.edu and cite “Probability Distributions for Carbon Emissions and Atmospheric Response” Clifford Singer, T.S. Gopi Rethinaraj, Samuel Addy, David Durham, Murat Isik, Madhu Khanna, Jianding Luo, Donna Ramirez, Ji Qiang,Wilma Quimio, Kothavari Rajendran, Jürgen Scheffran, T. Nedjla Tiouririne and Junli Zhang (manuscript in preparation).

Abstract: Probability distributions for future fossil carbon burning, atmospheric CO_2 concentration, and global average temperature change are produced by calibrating models of utility optimization, carbon balance, and heat balance against time series data. Utility optimization uses log-linear production functions for primary energy production and final gross domestic product (GDP). Population growth rates are used to calibrate an index of development that evolves logistically with time.

Energy production is a function that is log-linear in capital, labor, development, times a production efficiency coefficient that decreases linearly with decreasing carbon intensity of energy production. Carbon intensity is a piecewise linear function of fossil carbon depletion that is data calibrated for the past and determined by a tolerable threshold theory of international cooperation on future emissions limitations. GDP is log linear in capital, labor, energy, and development.

Atmospheric carbon and heat balance are determined by first order differential equations with carbon use rates and cumulative carbon use as drivers in the carbon balance and the greenhouse effect of increased atmospheric CO_2 as a driver in the heat balance.

Periodic oscillating corrections to all of these models are included where required to make residuals between data and model results indistinguishable from independently and identically distributed (iid) normal distributions according to statistical tests on finite Fourier power spectrum amplitudes and nearest neighbor correlations.

The evolution of an asymptotic approach to a sustainable non-fossil energy production is followed for a global disaggregation into a tropical/developing and temperate/more-developed region. In this context, the increase in the uncertainty of global average temperature evolves quadratically with the increase in the temperature from the end of the time–series calibration period through the next one and a half centuries.

-1-

I. Motivation:
Find Systematic, Time-Series Calibrated, Random Samples

Criteria for Exploratory Model Choice

Econometric model:
  Simple but theoretically complete
Atmospherics models:
  Laplace transform integrable for calibration
Empirically adequate:
  Residuals between data and theory “iid”
Computationally efficient:
  For parameter estimation and sampling
Parsimonious:
  Minimum number of free parameters
Data dominated:
  Minimally informative prior distributions
Data base and regional disaggregation:
  Flexible across time and space

II. Characteristics of Chosen Models

Dynamic optimization of $\int_{-\infty}^{t} dt\, a\, e^{-\rho\, t} (C/a)^{1-\theta} \big/ (1-\theta)$

$a = 1/(1 + \mathrm{Exp}[-\overline{\nu}\,(\tilde{t} - \overline{t}_0)])$ =Population $P(t)/\mathrm{Limit}_{\tilde{t}\to\infty}(P)$
Consumption $C = Y/\alpha - r\,K - \dot{K}$ =
production – depreciation – capital buildup $\dot{K}$

Two Sector Economies

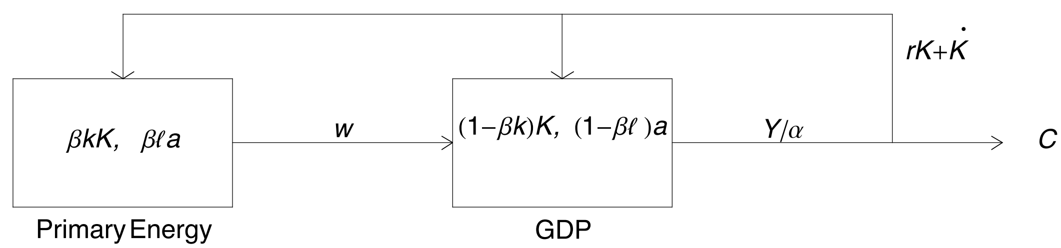

Log-linear GDP and primary energy production

$Y = (a^{\eta}\, ((1-\beta k)\, K)^{\alpha}\, ((1-\beta l)\, a)^{\omega})^{\varphi}\, w^{\beta}$
$w = p\, a^{\zeta}\, (kK)^{\alpha}\, (la)^{\omega}$ = Energy use rate
with constant returns to scale ($\alpha+\omega=\beta+\varphi=1$) for
labor $(1-\beta l)a$, βla; capital $(1-\beta k)K$, βkK; and w:

Energy production efficiency depends on
fossil carbon depletion: $p=1+(h-1)f$

Carbon intensity of energy production f declines
with fossil carbon depletion as in Fig. 7.

Atmospheric carbon and heat balance drivers with relaxation

$$d\tilde{C}/d\tilde{t} = \overline{B}\,\tilde{F}_{\rm net} + \overline{\beta}\,\tilde{E}_{\rm net} - \overline{\sigma}\,\tilde{C}$$
$$d\tilde{T}/d\tilde{t} = \overline{\mu}\,\mathrm{Ln}\left[1 + \left(\tilde{C}/\tilde{C}_0\right)\right] - \overline{\alpha}\,\tilde{T}$$

Carbon balance drivers are
Carbon emissions rate $\tilde{E}_{\rm net} = \eta_{\rm net}\overline{E}\ f\,\mathrm{w}$
Cumulative carbon emissions $\tilde{F}_{\rm net}$

Driver for global average temperature increase $\tilde{T}$ depends on
$\tilde{C}$ = atmospheric CO_2 concentration increase
$\tilde{C}_0$=277 ppm =preindustrial value (1700-1755)

No overbar/tilde symbols use dimensionless units:
Time in units of capitalization time $\overline{t}$=1/($\overline{r}+\overline{\rho}$):
{$\overline{r}$,$\overline{\rho}$}={depreciation,discount} rates in 1/yr
Capital in units of long-term limit total capital $\overline{K}$
Energy use rate in units of limit value $\overline{w}$
Carbon intensity in units of coal value $\overline{f}_1$
Carbon use rate E=$f\,w$ is in units of $\overline{E}=\overline{f}_1\,\overline{w}$

III. Solution Methods

Expand Euler-Lagrange equations in three sets of small constants to lowest order in
capital fraction of energy (β)
carbon depletion time / capitalization time
and through first order in $\overline{\nu}\overline{t} =$
capitalization time / development time

Then integrate fossil carbon balance : $\dot{u} = f\,\mathrm{w}$

This gives $k = l = 1$

and $\tilde{E} = \overline{E}\, a^{\psi}\, f\, p\, F^{\alpha/\omega}$ where

$F = (1 + \epsilon_1\, a)/(1 + \epsilon_1)$ and

$\epsilon_1 = \nu\,\theta\,\xi$ with $\xi = \zeta/\omega$

To find f solve the fossil carbon balance for $\tilde{u}$:

$$\mathrm{Ln}\left[\frac{(bh\,\overline{f}_k/\overline{f}_1)+1/(1-\tilde{u}\,\overline{m}_k/\overline{f}_k)}{(bh\,\overline{f}_k/\overline{f}_1)+1/(1-\overline{u}_2\,\overline{m}_k/\overline{f}_k)}\right] = \epsilon_k(\ S[a] - S[a_2]\ ) \quad \text{where}$$

$$S[a] = \int_0^a da\ a^{\psi}(1\text{-}z\,\epsilon_1\,\alpha/\omega)/(\ z\ a\ )$$

z=1-a and b=h–1

$\tilde{f}_k = \overline{f}_k - \overline{m}_k\,\tilde{u}$= piecewise linear Gtonne/EJ carbon
intensity vs. Gtonne carbon depletion

a_2=historically calibrated development index at break
between slopes $\overline{m}_2$ and $\overline{m}_3$ (c.f. Fig. 7)

⇒ $\tilde{E}$[S[a]] known in terms of standard analytic functions!

Note: Population, GDP, and primary energy solved for are increments over 1820 base values.

IV. Calibration

Periodic corrections to make residuals
between model and data apparently iid
(independently & identically distributed)

- Fit above "secular" model with least squares
- Discrete residuals Fourier series power spectrum
- Add sine and cosine corrections for dominant modes step wise until residuals appear iid

Maximum likelihood fits:

Under normal iid assumption for residuals δ_j,
integrate likelihood over σ

$$L = \int_{-\infty}^{\infty} d\mathrm{Ln}[\sigma] \prod_{j=1}^{n} \left(2\,\pi\, e^{2\,\mathrm{Ln}[\sigma]}\right)^{-n/2} e^{-(\delta_j/e^{\mathrm{Ln}[\sigma]})^2/2}\, P_{\mathrm{prior}}$$

Set P_{prior} uninformative, or log-normal for h, $B=\overline{B}\overline{\sigma}/\overline{\beta}$
and $\overline{\alpha}$ and compare results for standard deviations
σ_{prior}=0.2, 0.3, 0.4

Set ∂L/∂X =0 analytically when linear in X
and numerically otherwise

V. Sampling

For linear parameters:
  transform to uniform circle (in 2D) or hypersphere
    sample F distribution for radius
    uniformly sample around circle (or hypersurface)
For nearly linear parameters
    rejection sampling under multitvariate-t
For very nonlinear parameters
    successively sample 1-D marginal distributions

These sampling methods are also applied to
atmospheric balance equations, solved by:

- Laplace transforms of data for model calibration

$$\tilde{C} = \overline{C}_1 + e^{-\overline{\sigma}\,\tilde{t}} \int_{\tilde{t}_1}^{\tilde{t}} e^{\overline{\sigma}\,\tilde{t}} \left(\overline{B}\,\tilde{F}_{\mathrm{net}} + \overline{\beta}\,\tilde{E}_{\mathrm{net}}\right) d\,\tilde{t}$$

$$\tilde{T} = \overline{T}_1 + e^{-\overline{\alpha}\,\tilde{t}} \int_{\tilde{t}_1}^{\tilde{t}} e^{\overline{\alpha}\,\tilde{t}}\, \mathrm{Ln}\left[1 + \left(\tilde{C}/\tilde{C}_0\right)\right] d\,\tilde{t}$$

- Numerical differential equation integration for projections

VI. Key Robust Result

Uncertainty in future global average temperature grows quadratically with temperature increase:

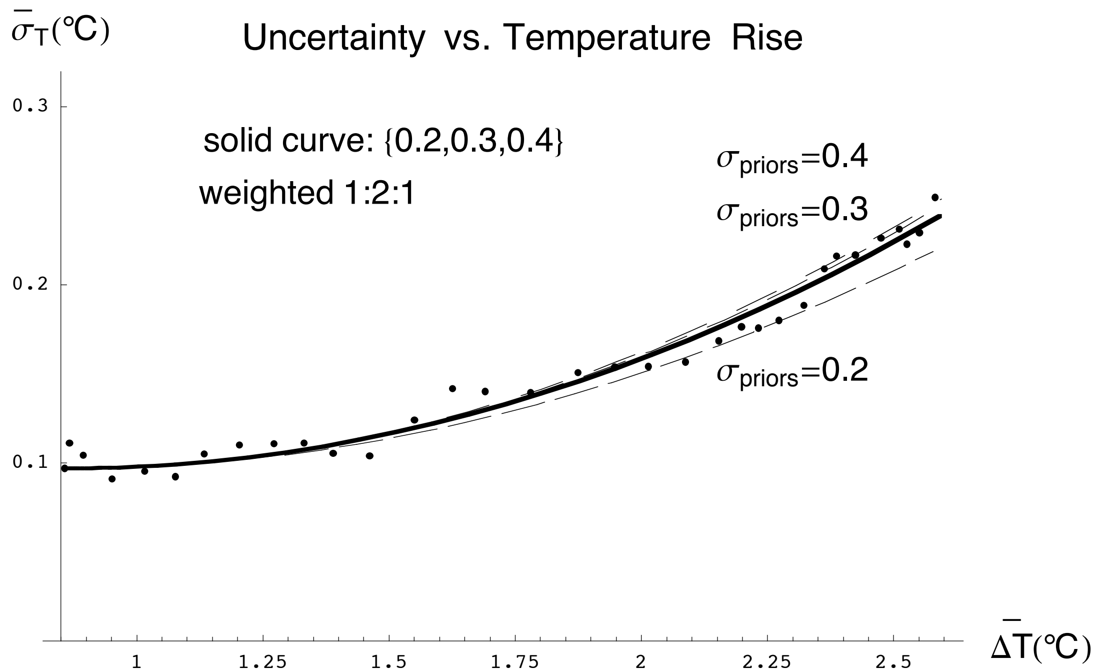

Fig. 1. Standard deviation $\overline{\sigma}_T$ versus mode for global average temperature increase $\overline{\Delta T}$ for quinquennially spaced fits of the type shown in Fig. 16d (dots, for σ_{priors}=0.3) and for quadratic fits to increases over year 2000 values from 2005–2160. Dashed curves are fits for the indicated standard deviations σ_{prior} for the carbon intensity slope changes shown in Fig. 11 and for h (the ratio of energy production efficiency for technologically advanced cheap fossils to that for non-fossils), $B=\overline{B}\,\overline{\sigma}/\overline{\beta}$ (the near surface CO_2 sink saturation parameter), and $\overline{\alpha}$ (the global average temperature relaxation coefficient). The solid curve is for a 1:2:1 weighting of results for σ_{priors}=0.2, 0.3, and 0.4.

VII. Regional Disaggregation

Temperate/Developed Region

Fig. 2. Geographical entities designated as temperate region if any part of territory lies poleward of 40 degrees latitude (Puerto Rico, Taiwan, and all of Korea are included with the geographical entities in this region).

Tropical/Developing Region

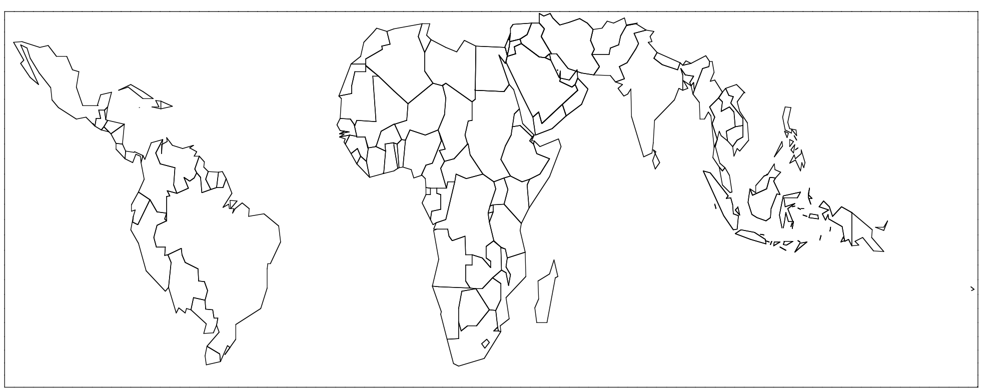

Fig. 3. The tropical region contains countries of which no part lies poleward of 40 degrees latitude.

VIII. Detailed Results

Table 1 shows econometric maximum likelihood estimates:

Tropical	Temperate.	Meaning
2001.6	1966.8	inflection time $\bar{t}_0$ (Julian yr)
0.0407	0.0517	development rate $\bar{\nu}$ (1/yr)
0.0180	0.0205	intercept $\bar{f}_3$ (Gtonne/EJ)
0.0165	0.0127	1000 × (slope $-\bar{m}_3$ in 1/EJ)
2.1251	2.0723	h=fossil/nonfossil productivity
1.7971	1.4442	ψ=dLnE/dLna
5.0964	7.0775	$\bar{E}$ scale (Gtonne/yr)
Derived		
24.585	19.353	development time $1/\bar{\nu}$ (yr)
0.0006	0.0005	$\epsilon_3=\bar{w}\bar{t}\bar{m}_3 \ll 1 \Rightarrow$ slow depletion
0.3155	0.4008	development rate $\nu=\bar{\nu}\bar{t}$
0.1791	0.5275	capitalization lag $\epsilon_1=\nu\ \theta\ \xi$
0.0186	0.1707	lag term $\gamma_2\,(\epsilon_1\,a\,(1-a))^2\,\vert_{a=1/2}$

The least accurate of the approximations made to produce analytic results is the neglect of the second order capitilzation lag correction $\gamma_2\,\epsilon_1\,a(1-a)$, which peaks at ~ 0.17 for the temperate region at the inflection point a=1/2 shown in Fig. 5.

Fig. 4 shows calibration of development index *a* against population growth rates

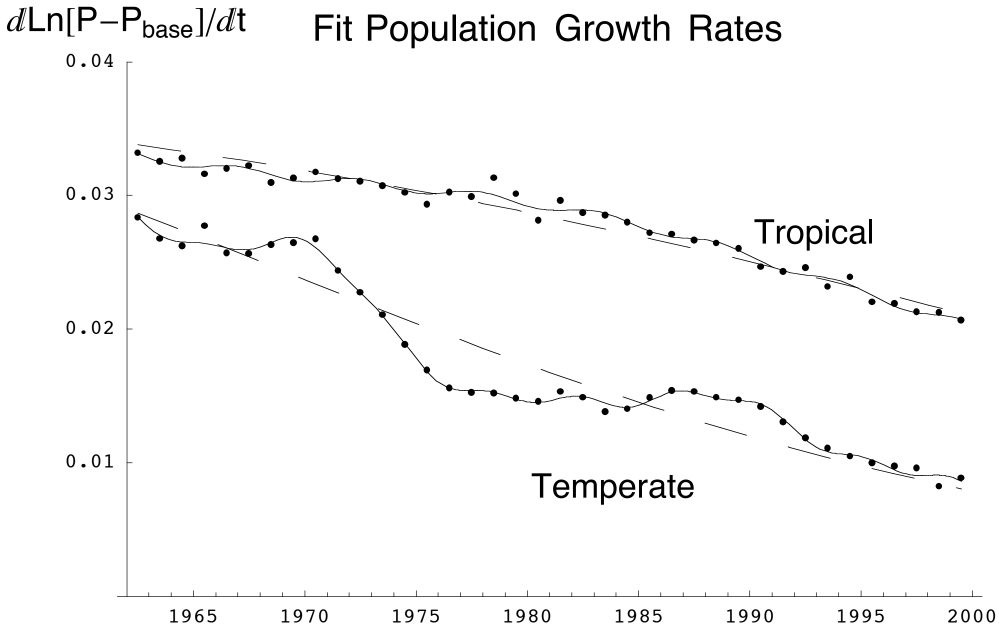

Fig. 4. Incremental population growth rates $\mathrm{Ln}[P - P_{\mathrm{base}}]/d\,\tilde{t} = \bar{\nu}\,z + \sum_{k=1}^{m} \bar{A}_k\,\mathrm{Sin}[\;2\pi(\tilde{t} - \bar{\tau}_k)/\bar{T}_k]$ where z = 1-a and a=$(1 + \mathrm{Exp}[-\bar{\nu}(\tilde{t} - \bar{t}_0)])$. The constants for the tropical region are P_{base}=0.37 billion, $\bar{\nu}$=0.0517 yr^{-1}, $\bar{t}_0$=1996.8 yr, m=2, 100$\bar{A}$={0.087,0.031}, $\bar{\tau}$-2000={-6.90,-1.80} yr and $\bar{T}$={38,38/7} yr. The constants for the temperate region are P_{base}=0.68 billion, $\bar{\nu}$=0.0407 yr^{-1}, $\bar{t}_0$-2000=-6.90 yr, m=5, 100$\bar{A}$={0.186, 0.139, 0.078, 0.068, 0.36}; $\bar{\tau}$={3.02,5.54,1.32, -0.37.0.35} yr; $\bar{T}$={38/2,38,38/4,38/3,38/9} yr. Dashed curves omit the periodic corrections.

Fig. 5 shows development index *a* and base and limit populations

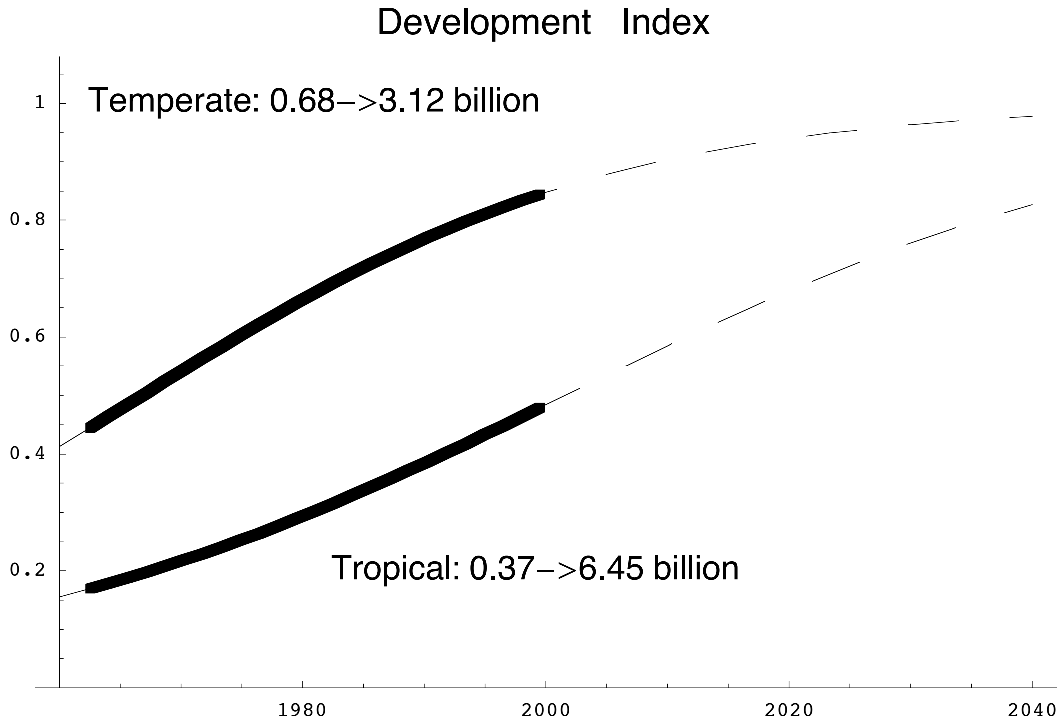

Fig. 5. Extrapolated development indices $a = (\tilde{P} - \overline{P}_{\text{base}})/(\overline{P}_\infty - \overline{P}_{\text{base}})$ for the indicated values of $\overline{P}_{\text{base}} \to \overline{P}_\infty$ Solid portions of the curves indicate the time range of the data stream used for calibration.

Fig. 6 plots development inflection date $\overline{t}_0$ samples vs. initial growth rate $\overline{\nu}$

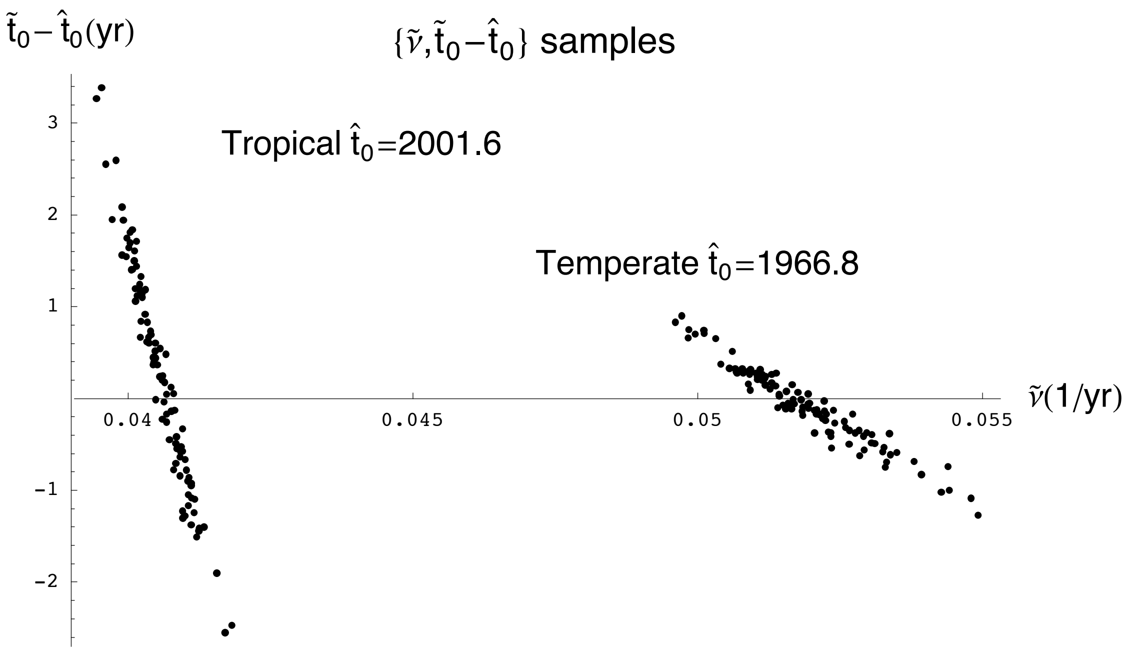

Fig. 6. Scatter plots of 100 random samples of initial development rate, with the indicated maximum likelihood estimates $\hat{t}_0$subtracted from inflection time samples $\overline{t}_0$ so that both regions can be plotted on the same graph.

Fig. 7 shows maximum likelihood and linear part of sampled fits to carbon intensity

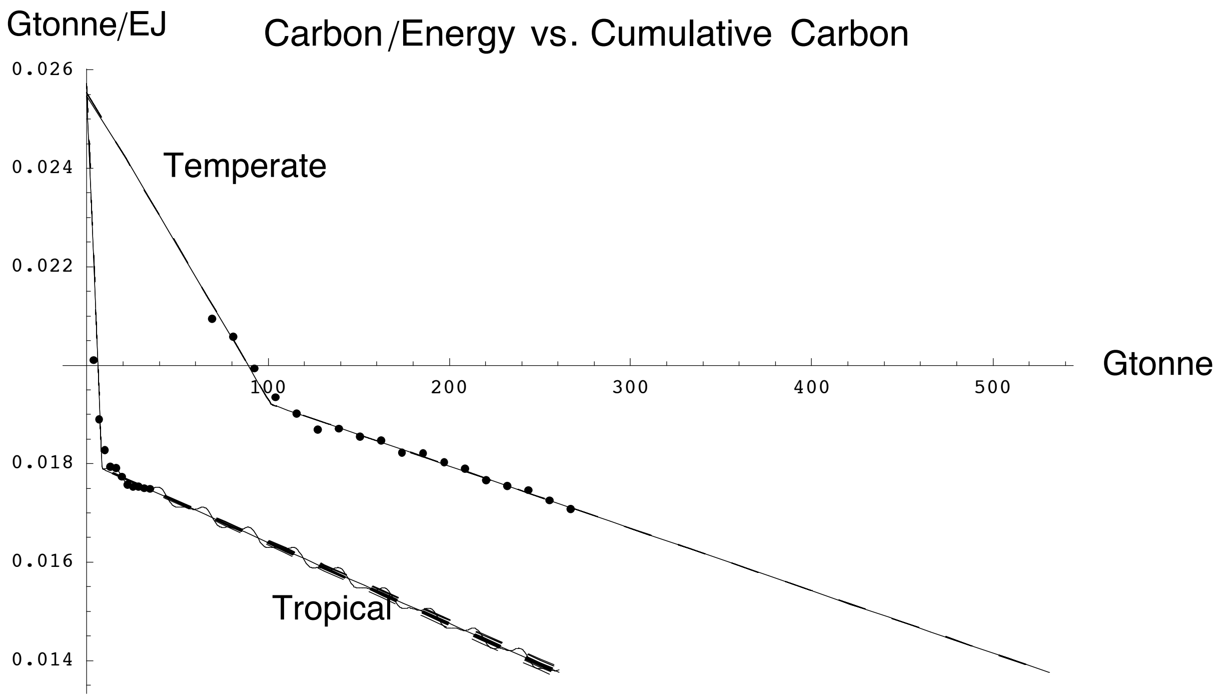

Fig. 7. Piecewise linear maximum likelihood fits (solid line and curve and sets of twenty random samples (dashed lines). A periodic correction $\sum_{k=1}^{2} \overline{A}_k$ Sin[$2\pi(\tilde{u}-\overline{\tau}_k)/\overline{T}_k$] is included for the maximum likelihood fit for the more recent potion of the tropical region (solid curve), with 100 $\overline{A}/\overline{f}_1$={0.41, 0.17}, $\overline{\tau}$={7.48, 12.86} Gtonne and $\overline{T}$={24.93, 12.46} Gtonne.

Fig. 8 gives maximum likelihood fit and sampling of carbon use rates. (Fitting is done to Ln[data] which gives more weight to small values.)

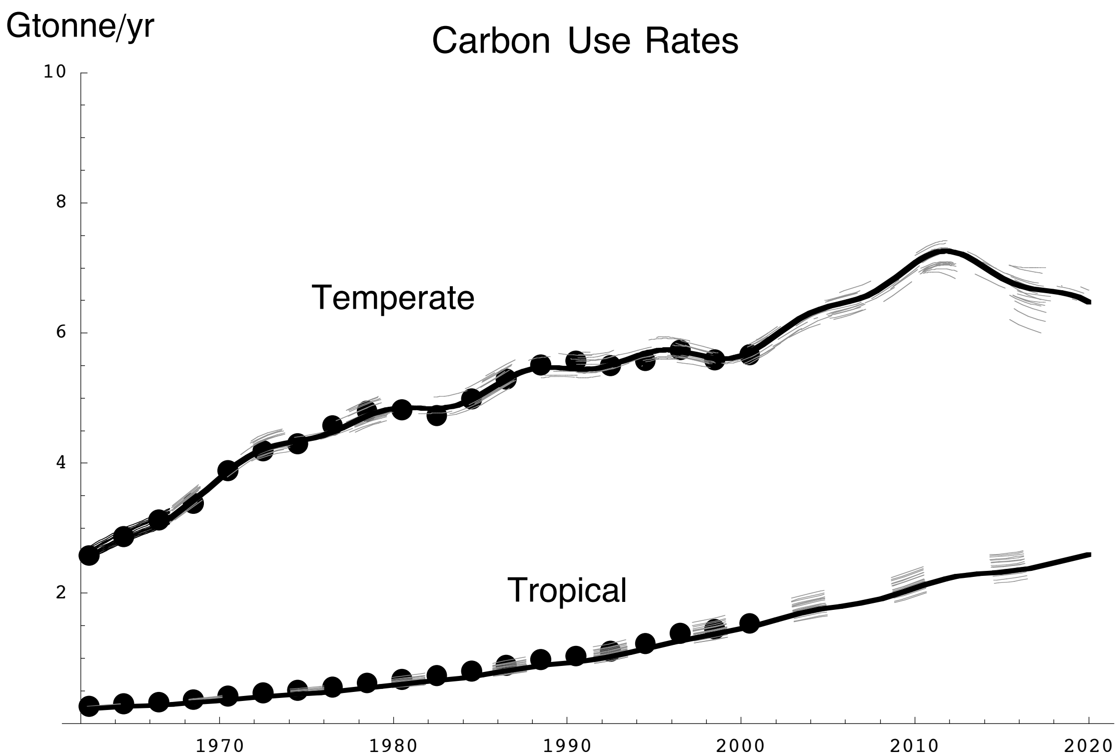

Fig. 8. Carbon use rate fits vs. biennially averaged data for maximum likelihood estimates (solid curves) and sets of twenty random samples (dashed curves). The solid curves multiply results using the secular parameters in Table 2 in the text by corrections of the form Exp[$\sum_{k=1}^{3} \overline{A}_k \,\mathrm{Sin}[2\pi(\tilde{t}-\overline{\tau}_k)/\overline{T}_k]$] where the period $\overline{T}_k$, phases $\overline{\tau}_k$, and amplitudes $\overline{A}_k$ for solid curves are listed in the upper part of Table 3.

Table 2 gives periodic corrections parameters:
~7% amplitude for temperate energy use is comparable to
~6% amplitude for Fig. 10 temperature periodicity

Tropical Emissions:			
Period (yr)	40.13	13.00	7.80
Phase (yr from 2000)	-2.72	2.93	1.92
Amplitude (%)	2.52	0.72	1.52
Temperate Emissions:			
Period (yr)	36.04	19.50	7.80
Phase (yr from 2000)	6.64	-3.41	1.72
Amplitude (%)	6.65	3.68	1.77
Global Temperature:			
Period (yr)	64.23	20.64	
Phase (yr from 2000)	5.90	-2.13	
Amplitude (°C)	0.101	0.044	

Fig. 9 samples fits to fractional increase in atmospheric CO_2.

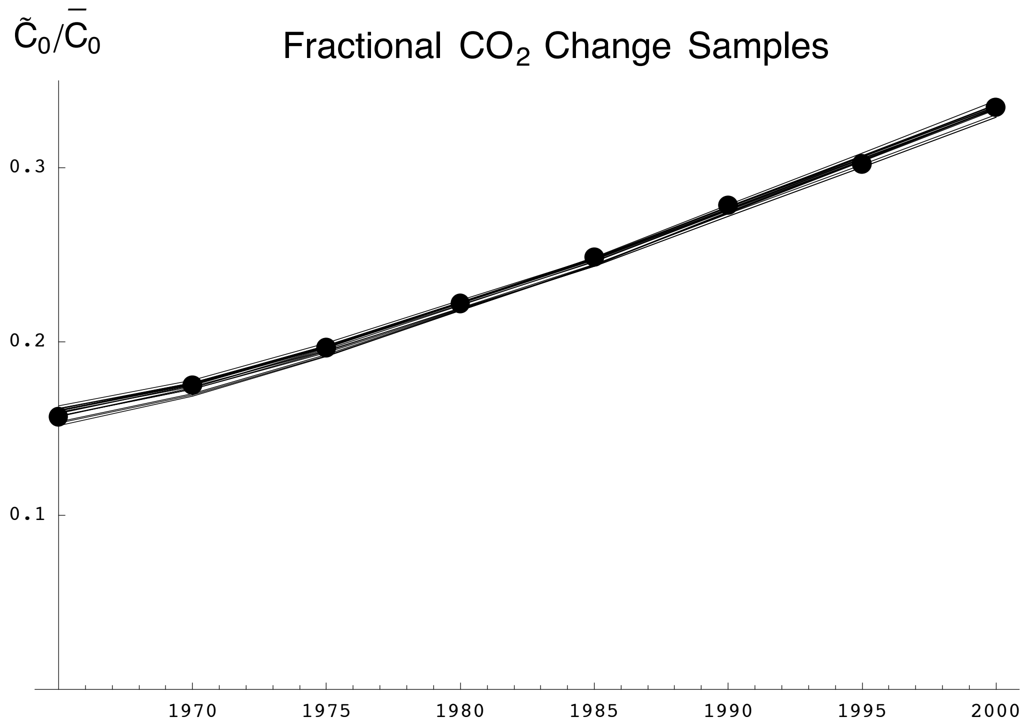

Fig. 9. Fractional change $\tilde{C}/\overline{C}_0$ of atmospheric CO_2 concentration plotted for quinquennially averaged data and twenty random samples. $\tilde{C}$ is the increment of CO_2 concentration over its preindustrial base value of $\overline{C}_0$=277 ppm.

Table 3 shows atmospherics maximum likelihood estimates.

Carbon:

Value	Meaning
0.0225	CO_2 relaxation coef. σ (1/yr)
0.0790	saturation coef. $B=\bar{B}/(\bar{\beta}\bar{\sigma})$
0.1095	$B=\bar{B}/(\bar{\beta}\bar{\sigma})$ prior mode (1/yr)
0.1482	$\tilde{C}/\bar{C}_0$ 1960 fit ($\Rightarrow$ $\bar{C}_0+\tilde{C}$=316 ppm)

Heat:

Value	Meaning
0.0171	thermal relaxation coef. $\bar{\alpha}$
0.0170	α prior mode (1/yr)
0.0979	greenhouse effect coef.(°C/yr)
-0.0040	base below lowest data (°C)

Fig. 10 samples fits to global average temperature change.

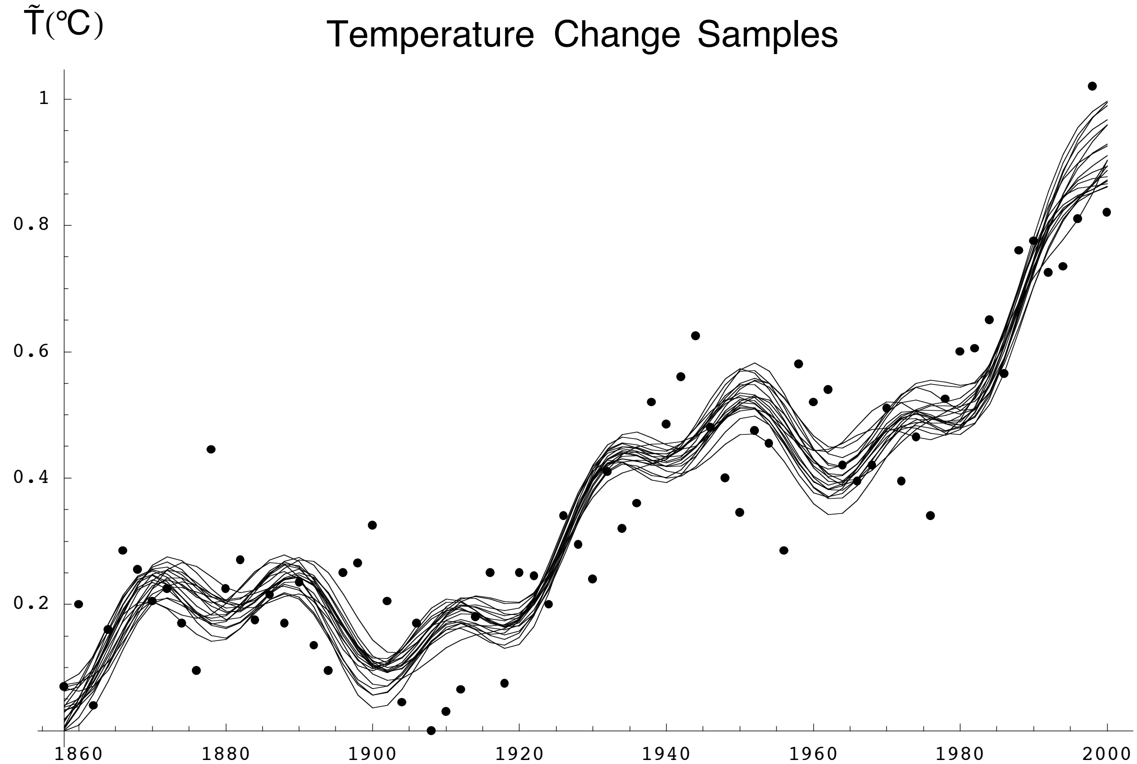

Fig. 10. Temperature increment over the lowest of the biennially averaged global average temperatures twenty random samples.

Fig. 11 samples past and future carbon intensity decline rates.

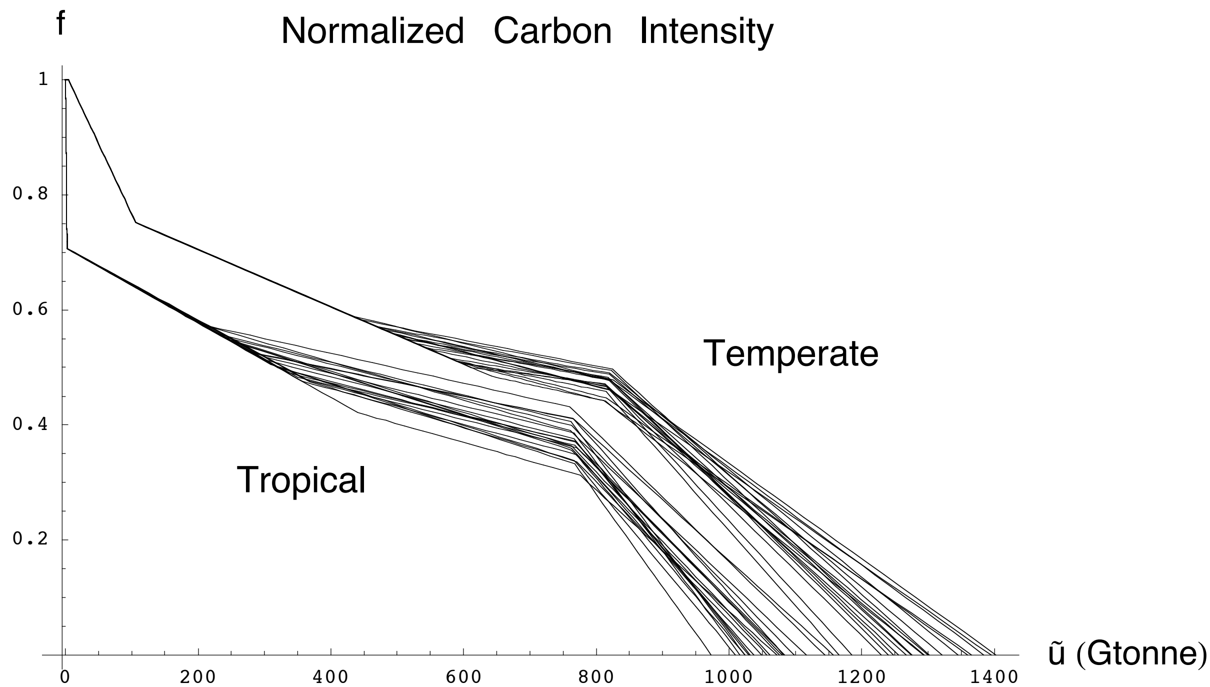

Fig. 11. Carbon intensity of energy production for sets of twenty random samples. A set of samples *d* is chosen from the standard log-normal distribution with mode and common standard deviation $\sigma_{\text{prior.}}$ The slope of the second decline from the right is sampled from data fits. This slope is divided by (1+ d) to model a "new age of coal" after the normalized carbon intensity has declined from its value $f_2$hat the first break between different downward slopes to $f_2 - (f_2 - f_{\text{gas}})d$ where f_{gas}=0.538 is the value for natural gas. The final slope is the second slope times (1+ d) and occurs when cumulative carbon use for each region exceeds a threshold of $\tilde{u}_3 + (800 - \tilde{u}_3)d$ where $\tilde{u}_3$is cumulative carbon use at the previous slope change.

Fig. 12 samples future global carbon burning.

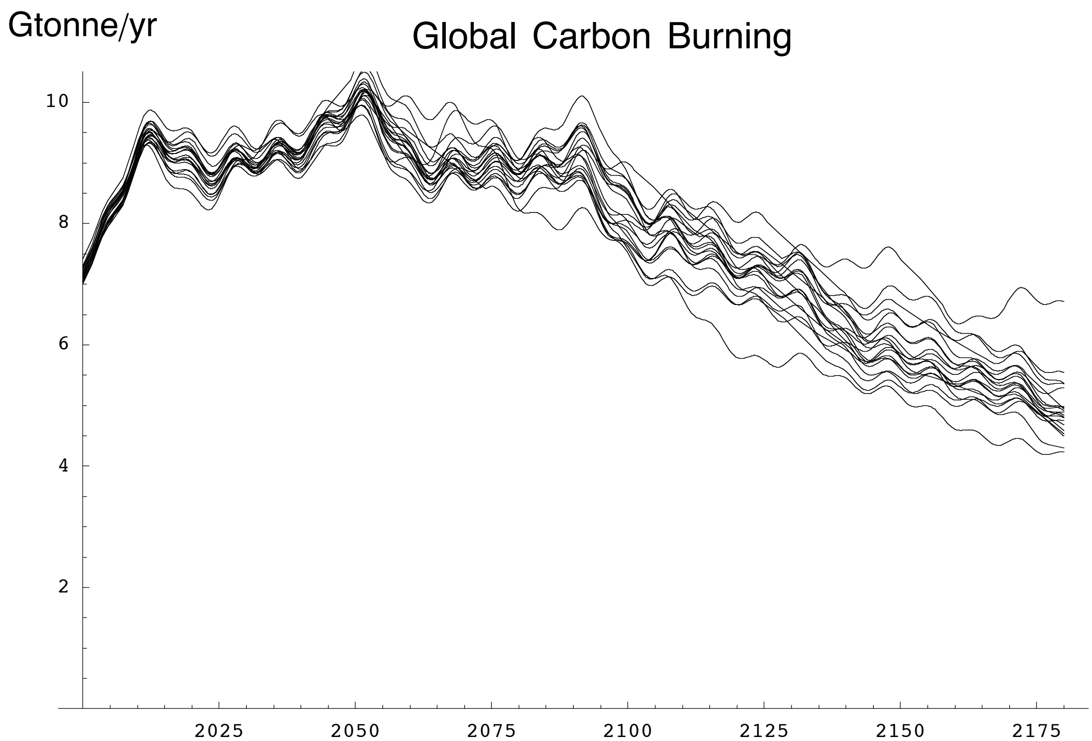

Fig. 12. Total global carbon burning for twenty random samples.

Fig. 13 samples cumulative carbon burning.

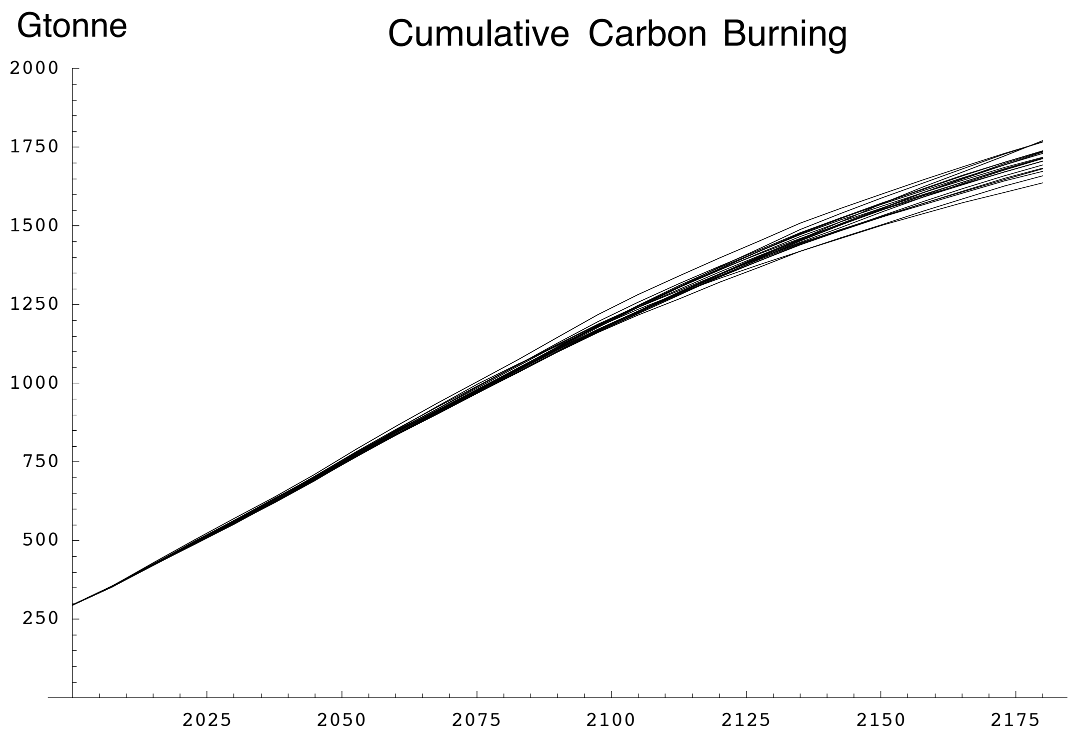

Fig. 13. Cumulative carbon burning for twenty random samples.

Fig. 14 samples future atmospheric CO_2 concentrations.

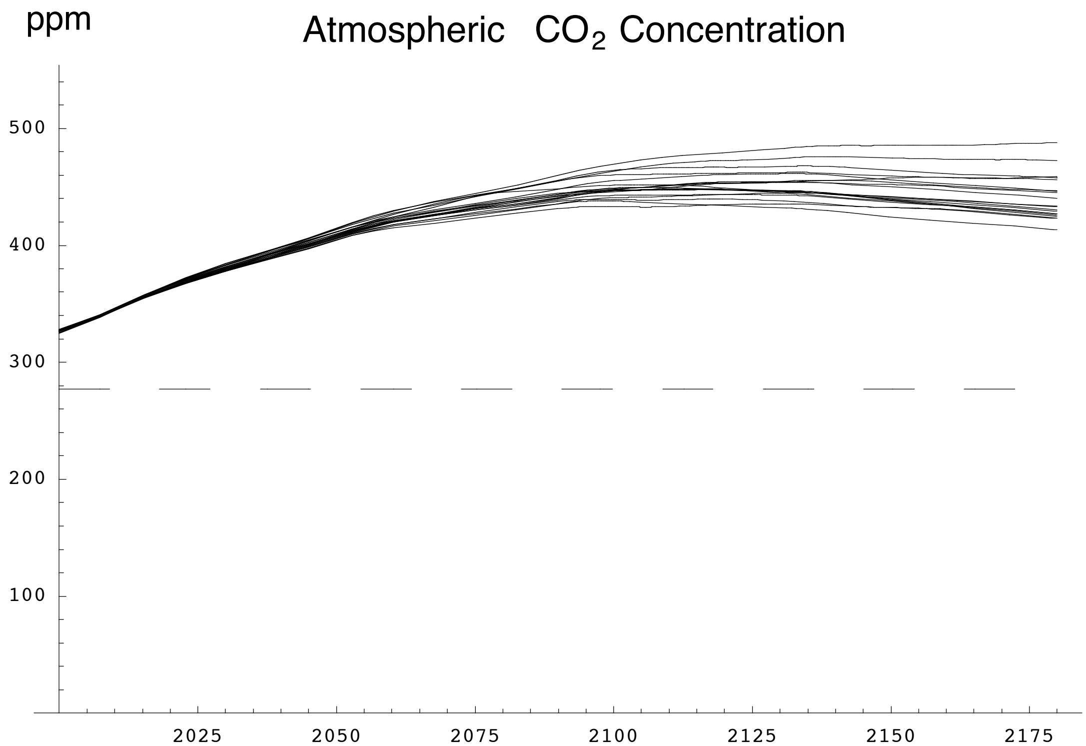

Fig. 14. Atmospheric carbon concentration for twenty random samples. The dashed line is the preindustrial base concentration.

Fig. 15 samples global average
temperature increase over preindustrial level.

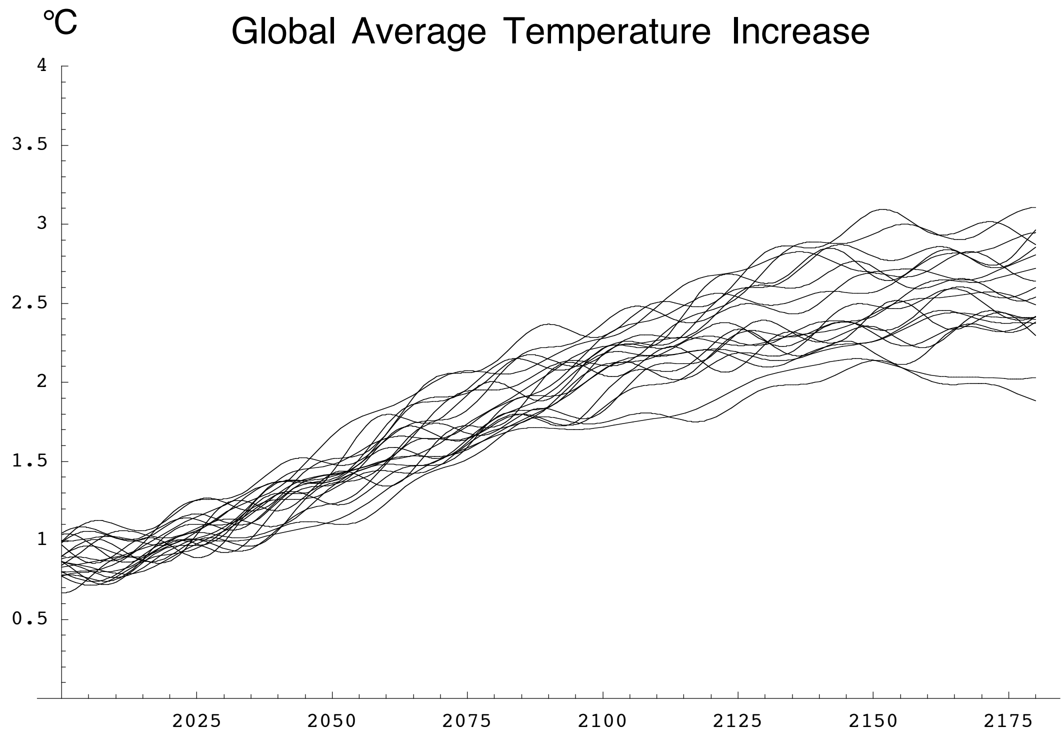

Fig. 15. Atmospheric carbon concentration for twenty random samples.

Fig. 16 shows normal fit to samples' cumulative centiles
(Such fits spaced at 5 year intervals provide the data points in Fig. 1.)

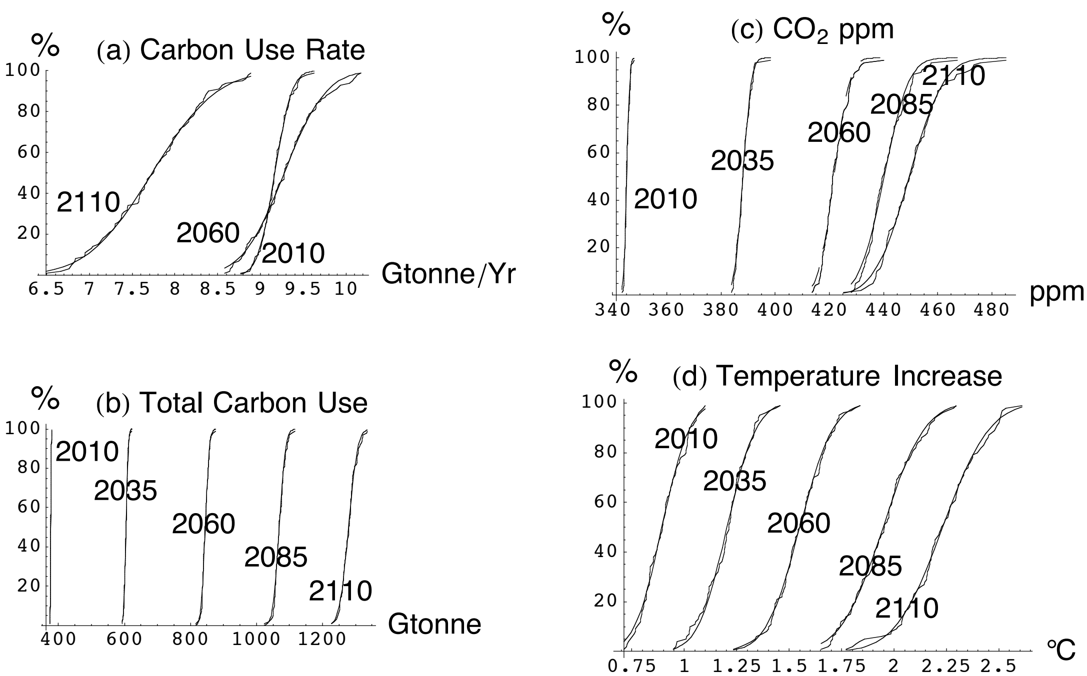

Fig. 16. Cumulative probability distribution centiles (jagged plots), and cumulative normal distributions fit to the central 95 centiles (smooth curves) for the indicated Julian years for global totals for (a) annual carbon use rate, (b) cumulative carbon use, (c) atmospheric CO_2 concentration, and (d) increase in average temperature due to anthropogenic carbon use.

Table 4 lists individual contributions to uncertainties

% of σ at			2060,2110,2160			
ppm CO_2			ΔT			
21	5	3	6	4	2	development
7	3	2	1	2	2	carbon/energy
48	21	15	9	11	9	burning
57	63	75	9	20	32	CO_2 balance
6	3	2	87	71	66	heat balance
34	30	21	3	12	12	new coal age
7	12	10	1	4	5	CO_2 reduction
6	28	44	1	4	18	carbon use limit

The largest contribution to uncertainties in CO_2 ppm comes from the carbon balance model.
Uncertainties in the emissions model make a comparable contribution for 2060.

Uncertainties in projected global average temperatures are dominated by uncertainties in the atmospheric heat balance model.
Uncertainties in the other models make only modest contributions (≤32%)

(Adding samplings successively until all are included gives 100% of the standard deviations σ, but the entries in Table 4 each resulted from adding one sampling to the maximum likelihood model and do not add linearly to 100%.)

IX. Why Is This Approach Useful?

- All significant model parameters are data calibrated

  (c.f. Table 1 for fixed global parameters)

- All parameters systematically sampled
  (residuals pass iid test for periodicity and nearest neighbor correlation)

- Any desired geographical aggregation and data range can be used.

- Time can be computationally efficiently fine gridded (e.g. down to annually).

- All time ($-\infty < \tilde{t} < \infty$) is covered starting from balanced growth

  from subsistence economies to sustainable nonfossil equilibrium

- Theory based models allow for conceptually based generalizations discussed below

Table 5 lists calibrated global parameters.

Value V	$\triangle V/V$	Type	Meaning
0.325	0.33	$0<\alpha<1$	capital share α
1.345	0.10	39	39 degrees freedom for θ
0.107	0.06	28	deprec. rate $\bar{r}$ in 1/yr
0.022	0.08	weighted	discount rate $\bar{\rho}$ in 1/yr
0.422	0.13	29	tropical dLnGDP/dLna
0.978	0.13	33	temperate dLnGDP/dLna
7.76		derived	capitalization time $\bar{t}$, yr

Data used are :
Labor shares of capital;
Satisfication / happiness survey vs. income;
U.S. depreciation rates;
Real interest rates vs. per capita GDP growth (c.f. Rethinaraj reference below)

X. What Improvements Would Be Useful?

- More complete long–term carbon balance model for physicochemically appropriate time-series-data calibrated sampling

- More complete treatment of greenhouse gases and heat balance to better isolate and sample “intrinsic” data–calibrated periodicities

- Finer regional disaggregation will require numerical integration or analytic approximation thereto forfast–growing economies (e.g. China)

- More complete theory of carbon intensity of energy production (e.g. shift from regional to global utility optimization when a threshold benefit is large enough to overcome vested interests opposing limitations on emissions)

Criteria for Prioritizing Improvements:

- For interpolating historical data and short–term projections, place emphasis on theory based models of non–random fluctuations (business cycles, cartel stability, other greenhouse gases and aerosols).

- For long term projections, develop prior probability distribution for theories of possible trends whose effects have not yet been manifest enough to be well constrained by data calibration (e.g. technology breakthroughs or development of global cooperationto end extreme poverty of the c. 1 billion people modeled here as subsistence population using very little primary energy).

- Systematic uncertainty analysis concentrates attention on what may be missing if the projected uncertainty seems intuitively too small and quantifies the most important features to be included in an adequate but parsimonious model.

XI. References—Methodology and Citations for this Work

Math methods used here require 4 references:
Box, G. E. P, and G. C. Tiao, *Bayesian Statistical Inference* (1972)
Wei, W. W. S., *Time Series Analysis* (1990),
Wolfram, Stephen, *The Mathematica Book* (2003)
Press, Frank, et al. *Numerical Recipes* (1986)

Atmospherics model prior probability distributions parameters:
Pethchel-Held, G., H-J. Schellnhuber, T. Bruckner, F. L. Tót, and K. Hasselmann K. "Tolerable Windows Approach: Theoretical and Methodological Foundations. *Climatic Change* **41** (1999) 303-331.

For derivations and to cite these ideas:
T.S. Gopi Rethinaraj, *Modeling Global and Regional Energy Futures,* University of Illinois at Urbana-Champaign PhD Thesis (2005).
“Probability Distributions for Carbon Emissions and Atmospheric Response, Clifford Singer, T.S. Gopi Rethinaraj, Samuel Addy, David Durham,Murat Isik, Madhu Khanna, Jianding Luo,Donna Ramirez, Ji Qiang,Wilma Quimio, Kothavari Rajendran, Jürgen Scheffran, T. Nedjla Tiouririne and Junli Zhang (manuscript in preparation).